Selective Molecular Annealing: *In Situ* Small Angle X-ray Scattering Study of Microwave-Assisted Annealing of Block Copolymers

Daniel T. W. Toolan,[1] Kevin Adlington,[2] Anna Isakova,[3] Alexis Kalamiotis,[2] Parvaneh Mokarian-Tabari,[4] George Dimitrakis,[2] Christopher Dodds,[2] Thomas Arnold,[5] Nick J. Terrill,[5] Wim Bras,[6] Daniel Hermida Merino,[6] Paul D. Topham,[7]* Derek J. Irvine,[2]* and Jonathan R. Howse[1]*

[1.] Department of Chemical and Process Engineering, University Of Sheffield, Sheffield, S1 3JD, UK.

[2.] Department of Chemical and Environmental Engineering, Faculty of Engineering, University of Nottingham, Nottingham, NG7 2RD, UK.

[3.] Department of Chemical Engineering and Applied Chemistry, Aston University, Birmingham, B4 7ET, UK.

[4.] Centre for Research on Adaptive Nanostructures and Nanodevices (CRANN) and AMBER Centre, Trinity College Dublin, Dublin 2, and Department of Chemistry, University College Cork, Ireland.

[5.] Diamond Light Source Ltd, Harwell Science and Innovation Campus, Didcot, OX11 0DE, UK.

[6.] Netherlands Organisation for Scientific Research, DUBBLE@ESRF Beamline BM26, ESRF - The European Synchrotron, 71, Avenue des Martyrs, CS 40220, 38043, Grenoble Cedex 9, France.

[7.] Aston Institute of Materials Research, Aston University, Birmingham, B4 7ET, UK.

Abstract:

Microwave annealing has emerged as an alternative to traditional thermal annealing approaches for optimising block copolymer self-assembly. A novel sample environment enabling small angle x-ray scattering to be performed *in situ* during microwave annealing is demonstrated, which has enabled, for the first time, the direct study of the effects of microwave annealing upon the self-assembly behavior of a model, commercial triblock copolymer system [polystyrene-*block*-poly(ethylene-*co*-butylene)-*block*-polystyrene]. Results show that the block copolymer is a poor microwave absorber, resulting in no change in the block copolymer morphology upon application of microwave energy. The block copolymer species may only indirectly interact with the microwave energy when a small molecule microwave-interactive species [diethylene glycol dibenzoate (DEGDB)] is incorporated directly into the polymer matrix. Then significant morphological development is observed at DEGDB loadings ≥ 6 wt%. Through spatial localisation of the microwave-interactive species we demonstrate, targeted annealing of specific regions of a multi-component system, opening routes for the development of "smart" manufacturing methodologies.

Introduction

Block copolymers (BCPs) are highly versatile materials finding wide ranging applications in the bulk such as adhesives, footwear, textiles and automotive components (commercial examples include: Kraton™, Solprene™, Hytrel™, Engage™, Sofprene™) and in thin-films for lithographic templating and materials for organic electronics, to name but a few.[1-4] BCPs comprise covalently bound polymer segments that are often immiscible with one another, which if given sufficient mobility, will phase separate on the molecular level to self-assemble towards an equilibrium state. This will result in the formation of well-defined highly ordered morphologies (such as cubic, hexagonal and lamellar) with characteristic length scales in the 10 – 100 nm range, *via* a process called 'microphase separation', for further details see selected references.[5-18] The versatility of BCPs arises from the potential to tune their self-assembly behaviour to achieve targeted morphologies, through controlling both their chemical composition (i.e. polymer-polymer interaction parameter, ratio of statistical segment lengths and the overall degree of polymerisation)[19, 20] and the kinetic processing pathway.[21-24]

Many techniques employed to process BCPs generate 'quenched' non-equilibrium morphologies, kinetically trapped far from thermodynamic equilibrium.[22, 25, 26] Consequently, to achieve highly ordered nanoscale structures, an annealing process is needed where heat (or solvent vapour) is employed to impart polymer chain mobility within the BCP to enable nanoscale molecular level rearrangement. [3, 26-32]

Microwave annealing of BCPs has recently emerged as a novel technique for optimising[20] nanostructures significantly faster than traditional thermal annealing approaches. [33-37] However, polymers themselves are inherently poor at interacting with microwave energy.[35, 38-40,41] Thus it has been postulated that the mechanism responsible for this accelerated annealing of BCPs must rely upon the presence of other species within the system, which possess a greater ability to interact with the microwave energy (e.g. supporting substrate or solvent/non-solvent) to produce a thermal effect. [35,41, 42] Jin and co-workers studied substrate dependant microwave annealing of BCP thin-films using both microwave interacting (silicon) and non-interacting (glass) substrates, using microwave compatible thermal probes. Their work conclusively showed that BCP annealing only occurred in the presence of a microwave interactive material.[41]

Presently we do not fully understand, and are unable to rationally optimise microwave annealing methodologies due to the constraints of conventional microwave cavities, which limit experimental observations of self-assembly. Consequently morphological development has typically been performed *ex situ.*[33-37] The dynamic nature of self-assembly processes make such experimental approaches far from ideal, necessitating trial-by-error procedures and the need to infer information

on how morphological development proceeded from the end point alone. As such, developing methodologies that enable self-assembly processes to be monitored *in situ*, are essential for both fully understanding microwave annealing approaches and allow the rational design of processing routes.

The details of microwave heating are discussed in detail in the ESI. In brief, the key to microwave heating is that to interact with microwave energy there must be an uneven distribution of electrons (such as dipoles or charge pairs) within a molecule, which must be free to move in response to the phase of the incident electromagnetic field. Whilst, both substrate and solvent-induced microwave annealing approaches have been successfully applied to thin-film systems, such approaches are inherently incompatible with bulk BCP materials as substrate heating relies on conductive/convective energy transfer from the substrate to the polymer, whilst solvo-microwave annealing requires the diffusion of solvent molecules into the polymer matrix to deliver annealing *via* microwave selective heating. In thin films both of these processes are rapid due to the high surface area to volume ratio, whilst in the bulk, diffusion processes occur on much longer timescales.

The study herein, presents the first *in situ* observations of nanoscale morphological development induced by microwave annealing, utilising a highly novel sample environment that enables small angle x-ray scattering (SAXS) to be performed *in situ* on a sample placed inside a microwave cavity (shown schematically in Figure 1).[43] This experimental technique was used to demonstrate a new microwave annealing approach applied to a model, commercial triblock copolymer system [Kraton G1652; polystyrene-*block*-poly(ethylene-*co*-butylene)-*block*-polystyrene (SEBS)], based upon the incorporation of a microwave-interactive small molecule additive [diethylene glycol dibenzoate (DEGDB)] directly into the polymer matrix. It is well reported that Kraton G1652 may form a non-equilbrium nanostructure consisting of lamellar microdomains and upon annealing an equilibrium nanostructure of hexagonally close packed domains of PS cylinders is obtained.[21, 44-47] The DEGDB small molecule additive may be incorporated as either a homogenous or localised microwave interactive species, within the BCP material that enables the microwave unresponsive material to interact with microwave energy, resulting in heating and consequent annealing of bulk BCP nanostructures. This new approach demonstrated here circumvents the drawbacks associated with substrate and solvent microwave annealing approaches that restrict applications beyond thin-films. Furthermore, we introduce and demonstrate a methodology to enable selective annealing of different regions of a multi-component (layered), mixed copolymer system based upon the location and partitioning of the microwave interacting species. Hence, such an approach opens routes to develop novel "smart" manufacturing, based on selective processing of specific zones

within the bulk of a material. Additionally, this approach presents the ability to optimise the local nanostructure of individual components or discrete areas of a system independently from other elements within a complex two or three dimensional structure.

Experimental

Sample preparation

G1652 and G1657 was kindly supplied by Kraton Polymers Belgium and was used as received. Kraton G1652 is a SEBS copolymer containing 30 wt% PS, with a number-average molecular weight (M_n) of 55.8 kg mol^{-1}, polydispersity index of (M_n/M_w) of 1.01. Kraton G1657 is a blend of SEB and SEBS copolymers, containing 13 wt% PS, with two distinct molecular weight species at 55.6 and 109 kg mol^{-1}, with polydispersity indices of 1.02 and 1.08, respectively. GPC traces are shown in Figure S5 ESI. Polymer solutions (Kraton G1652 & Kraton G1657) were made up at 10 wt% in THF and dissolved overnight, before the appropriate quantity of diethylene glycol dibenzoate (DEGDB) was added and homogeneously mixed. The solutions were subsequently cast into PTFE wells to afford films with a thickness of approximately 1.5 mm.

Microwave annealing

Parallel microwave annealing with *in situ* SAXS measurements were performed using a custom built rig integrated to the BM26B-DUBBLE beamline, which is shown schematically in Figure 1. The samples were prepared as described above and attached to a microwave transparent PTFE frame using Kapton tape, such that it was suspended over the aperture with minimal contact with the PTFE holder.

It is worth noting that the interaction of a material with microwave energy depends upon both the frequency of microwave energy and the shape of the cavity in which the microwave energy propagates. Here, we have made use of a single-mode cavity in which a single microwave propagates along the cavity, and is reflected by the short-circuit at the end of the cavity to create a standing wave. Microwave annealing was performed at 2,450 Mhz, which was the allocated ISM (Industrial, Scientific & Medical) microwave frequency for the study herein and the same as commonly used for large scale industrial and domestic applications.

The PTFE sample holder was inserted into the microwave cavity and impedance matching was performed using a Rohde & Schwarz ZVH8 portable network analyser through altering the position of the short-circuit and raising and lowering the tuning stubbs, to create an anti-node at the sample position and hence maximum energy absorption. The sliding short and stub tuners were adjusted to enable; (a) the level of reflected power within the system to be minimised and (b) the true level

of forward and reflected power to be recorded and thus the actual power absorbed by the sample to be calculated.

Following this, parallel microwave annealing with *in situ* SAXS measurements were performed. SAXS measurements were collected for a period of 20 seconds prior to microwave treatment to capture the morphology of the as-cast polymer sample. 200 W of microwave power was then applied 20 minutes after which the film was allowed to cool in the cavity for a period of five minutes.

Thermal annealing

For the *in situ* thermal annealing SAXS experiments, an custom built multi-sample rig was employed, comprising a stainless steel plate sandwiched between two ceramic insulating plates with 22 periodically placed 6 mm diameter apertures (to allow the x-ray beam to pass through in transmission). Samples were loaded into the apertures and encased by two single layers of Kapton tape. Data acquisition commenced at room temperature, before the samples were heated using Kapton film heaters (Omega) fixed to the stainless steel plate, to 150 °C for 7 hours and then passively cooled for approximately one hour.

Small angle x-ray scattering

In situ microwave annealing and thermal annealing small angle x-ray scattering experiments (SAXS) were performed in transmission at BM26B-DUBBLE beamline (λ = 1.033 Å, sample to detector distance of 3.5 m using a Pilatus 1M 981 × 1043 pixel detector with pixel size 172 μm) at the European Synchrotron Radiation Facility (ESRF), Grenoble, France.

Essential preliminary studies for this work were performed on I07 and I22 beamlines at the Diamond Light Source, Rutherford, UK.

GPC

Molecular mass data were obtained by Gel Permeation Chromatography (GPC) (flow rate 1 ml/min, 40 °C) using a Varian GPC spectrometer comprising three PL gel 5 μm 300 x 7.5 mm mixed-C columns and a degassed THF eluent system containing triethylamine (2 % v/v) and BHT (0.05 % w/v). The samples were calibrated with narrow polystyrene standards (M_p range = 162 to 6035000 g/mol) and analysed using PL Cirrus software (version 2.0) supplied by Agilent Technologies.
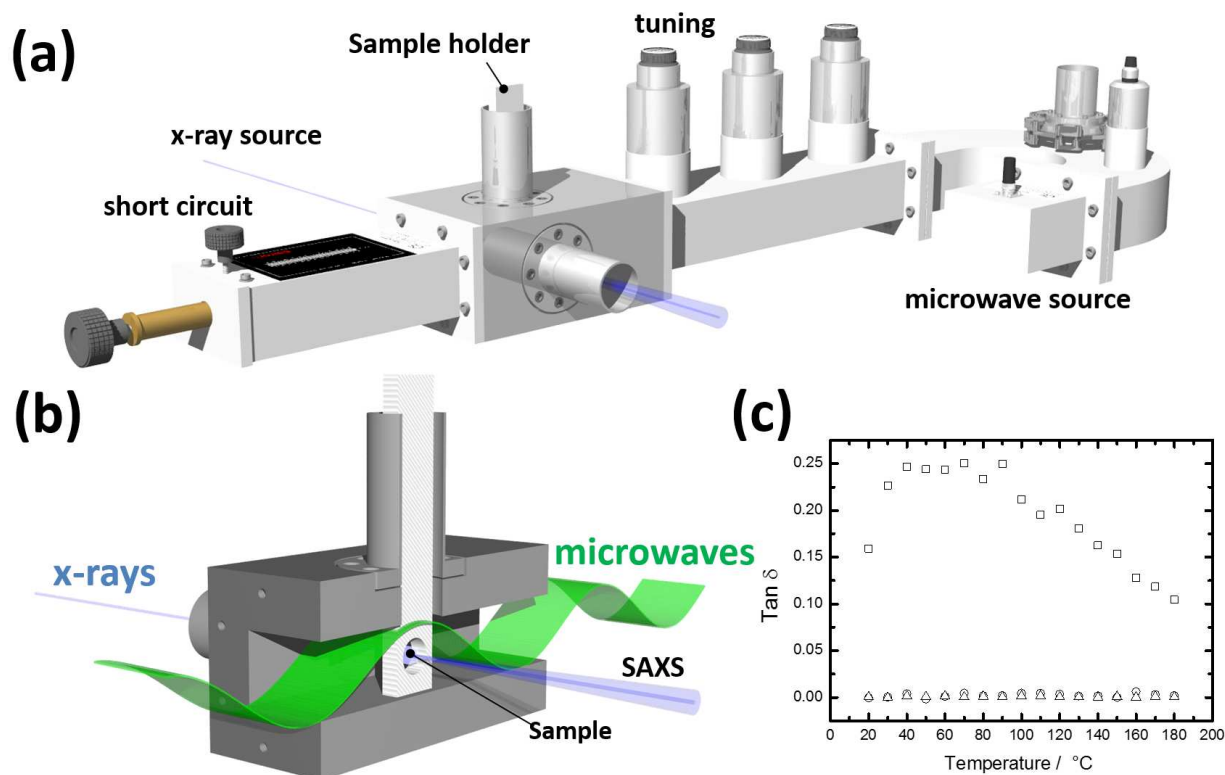
Figure 1: Schematic of the custom-built *in situ* x-ray scattering/microwave annealing rig, where (a) shows the complete constructed apparatus, (b) illustrates the sample environment within the TE10$_n$ single mode cavity integrated onto the x-ray beamline (*N.B.* sample is located at the maxima of the electric field) and (c) a plot of the variation of tan δ (See main text for definition) as a function of temperature for DEGDB (squares), Kraton G1652 (circles) and G1657 (triangles).

Results and discussion

In situ SAXS experiments were performed during microwave heating/treatment of the G1652 SEBS copolymer with a range of different DEGDB additive loadings (0 to 8 wt%) to evaluate the use of DEGDB as a microwave-responsive, molecular energy target; the radially integrated SAXS profiles [intensity (I(q)) *vs* q] is presented in Figure 2a. The data show that the as-cast samples exhibit prominent 1st, 2nd and 3rd order scattering features, with q/q^* ratios of 1:2:3, commensurate with the presence of lamellar microdomains, in agreement with the literature for this polymer.[21] The addition of DEGDB (2 – 8 wt%) to the bulk polymer matrix was found to not significantly alter the radially integrated SAXS profiles of the as-cast films.

The relatively high degree of order observed for the as-cast films was attributed to the slow evaporation of solvent during casting, required to generate relatively thick (0.5 mm) films suitable for this study. For the samples loaded with low amounts of DEGDB (0, 2 and 4 wt%), minor shifts in the radially integrated SAXS profiles were observed when the samples were microwave-treated/heated for a period of twenty minutes at 2,450 MHz. These small shifts do not represent any significant development of the lamellae nanostructures and indicate that without, and at low additive loadings the energy transfer upon microwave treatment/heating is not of sufficient magnitude to promote polymer chain mobility. So there is no notable change and increase in the order of the lamellae microdomains.
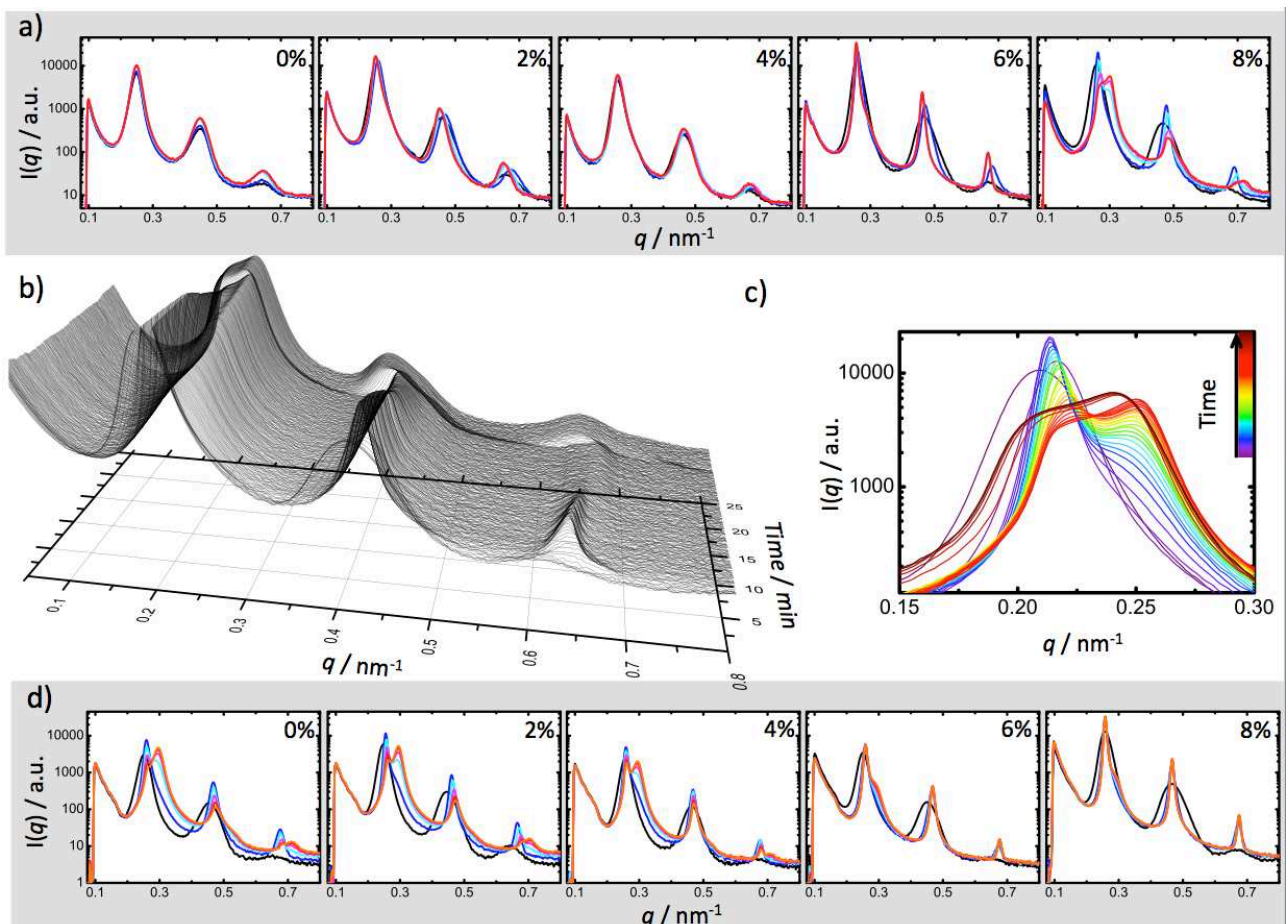

Figure 2: *In situ* SAXS data during microwave annealing, where (a) shows 1D radially integrated data for G1652 SEBS with different loadings of DEGDB absorber (0, 2, 4 6 and 8 wt%) at different microwave exposure times: 0 (black), 1.5 (blue), 7.25 (cyan), 13 (magenta) and 18.75 (red) minutes; (b & c) time-resolved 1D radially integrated

data for G1652 SEBS with 8 wt% DEGDB absorber; (d) shows 1D radially integrated data for G1652 SEBS with different loadings of DEGDB absorber (0, 2, 4 6 and 8 wt%) thermally annealed at 150 °C for: 0 (black), 1.5 (blue), 7.25 (cyan), 13 (magenta), 18.75 (red) and 24.5 (orange) minutes.

For higher DEGDB additive loadings (6 wt%) a significant sharpening of the lamellae peaks is observed upon microwave treatment/heating. Such peak sharpening is commensurate with increased order of the lamellae microdomains. In addition, at 7.25 minutes a weak feature emerges at q = 0.250 nm^{-1}, which is ascribed to the emergence of hexagonally close packed cylinders (HCP), as shown for thermally annealed G1652 SEBS.[21] The intensity of this peak only slightly increases upon the microwave treatment/heating, indicating that the bulk morphology of the G1652 SEBS with 6 wt% additive largely comprises of well-ordered lamellae microdomains with a small proportion of hexagonally packed cylinders.

The G1652 SEBS sample loaded with the highest amount (8 wt%) of DEGDB shows the most dramatic morphological evolution upon microwave treatment/heating. As such, the scattering behaviour of this sample is presented in more detail in Figure 2b and c. Upon application of microwave treatment/heating the lamellae peaks undergo rapid sharpening, reaching a maximum intensity and sharpness within two minutes, indicative of high mobility within the sample. After this period, the intensity of the lamellae peaks begins to decrease, coinciding with the emergence of the 1st order HCP peak. As the microwave treatment/heating continues, the magnitude of the HCP peaks increases with a commensurate decrease in the magnitude of the lamellae peaks (shown in more detail in Figure 2c), indicative of a transformation of the lamellae domains into hexagonally close packed cylinders.

These results clearly demonstrate that when G1652 is subjected to microwave treatment/heating (200 W applied), significant morphological development occurs only at sufficiently high additive loadings (≥ 6 wt%) and that at low additive loadings little energy transfer (and any consequent morphological development) takes place. Differential scanning calorimetry (DSC) was used to investigate the effect of DEGDB loading on the mobility of G1652, with data showing (SI Figure S3) that the T_g of the ethylene-butylene block lies between -56 and -57 °C (consistent with literature

values[48]) and does not appear to alter with addition of DEGDB at these loadings. The DSC traces do not show a clear T_g for the PS block, for either native and the BCP doped with DEGDB.

In order to validate the microwave annealing approach presented in Figure 2, comparative *in situ* thermal annealing SAXS experiments were performed on identical additive-loaded G1652 SEBS copolymers. Figure 2d presents radially integrated SAXS data acquired when G1652 SEBS samples loaded with varying levels of DEGDB (0, 2, 4, 6 & 8 wt%) were thermally annealed at 150 °C. Data are presented at the same time intervals as those in Figure 2a, to allow direct comparison between microwave and thermal annealing processing. The data presented in Figure 2d show that when thermally annealed, independent of additive loading, all exhibit an initial sharpening of the lamellae peaks, again indicating mobility, followed by the emergence of the 1st order HCP peak. Interestingly, the relative ratio between the lamellae and HCP scattering features decreases with increasing additive loadings.

To understand in detail how G1652 and DEGDB respond when subjected to microwave treatment/heating, their dielectric properties were measured *via* a cavity perturbation technique.[49-52] This enabled the prediction of the relative capability of the materials to contribute to system heating, when introduced to an electric field, so as to ensure that it was pre-designed toward achieving selective microwave heating (full details available in the ESI). In regard to microwave heating methods, the dielectric constant (ε') of a material indicates its ability to interact with and store energy from an alternating field, whilst dielectric loss (ε'') gives information on how readily/efficiently a material can convert an amount of the stored energy into heat or promotion of a chemical transformation. When a mixture of several different materials is placed within an electromagnetic field, the material with the higher dielectric properties typically has a greater potential to couple with the alternating field, and thus undergo selective heating.[53] However, comparison of the loss tangent (tanδ) values, which is defined as the ratio of the dielectric loss factor (ε'') and the dielectric constant (ε'), is typically used to predict the relative capability of the

material to contribute to the heating of the medium and/or enhancement of a chemical transformation when introduced to an electromagnetic field. The tanδ data for G1652 (Figure 1c & Figure S1 ESI) show that the BCP has essentially no ability to translate any microwave energy that is absorbed into heat, whilst DEGDB exhibited achieve this across a large temperature range (25 to 180 °C). These findings are attributed to the polymeric, physical form of G1652 that prevents the material from interacting with the microwave energy as the dipoles are heavily constrained as part of an extended microstructure and therefore it is difficult for them to align with the phase of the electromagnetic field. Thus, they fail to achieve the molecular motion required to translate this energy into heat. To further validate these findings and to ensure that the dielectric properties of the polymer do not appreciably change in the presence of a low molecular weight species, a sample of the polymer was dissolved into toluene, which is known to have a very low level of interaction with microwave energy. The dielectric properties of the polymer:toluene mixture were assessed and compared to that of the toluene alone and are presented in the ESI, Figure S2. The data show that the dielectric properties of the toluene:polymer mixture are essentially that of the toluene component. Thus, we are able to conclude that the presence of a low molecular weight, non-microwave absorbent moiety does not result in the polymer becoming more interactive due to a greater level of solvation and mobility. Rather, the restrictions imposed by the polymer chain still control its response to the electromagnetic field, thus the polymer should not selectively heat and so would not be likely to anneal by the direct application of microwave energy in the presence of low molecular weight, microwave transparent additives. Therefore, for the *in situ* SAXS data reported in this paper, any differential behaviour is solely related to the properties of the microwave interactive additive and the level of heating that would be achieved by its addition to the polymer, which is corroborated by the data obtained for 0 wt% DEGDB.

In addition, assessment of the dielectric properties enables calculation of the penetration depth of the electromagnetic field (as given by Equation S1 in the ESI). The penetration depth is defined as the point at which the electric field decays to e^{-1} of the value at the surface and is inversely proportional to the level of microwave absorbance that is exhibited by the material/mixture being

heated. Thus, the worst case scenario for penetration would be with 100% DEGDB, as it is the most microwave absorbent of the species used. The penetration depth was predicted as 2.45 cm (at 2450 MHz, see ESI for further details) and this defines that for the sample size of film employed in the work herein, the entire sample will be evenly treated by the incident microwave energy.

The approach of exploiting a small molecule additive as a homogenous microwave interactive species to anneal a BCP has been further demonstrated for Kraton G1657, which is a blend of SEBS and SEB copolymers, with results presented in the ESI, Figure S4. As predicted (from the results of Kraton G1652 presented herein), at low additive loadings the SAXS data show that there is no change in the morphology upon microwave treatment/heating, whilst in the presence of DEGDB clear morphological development of the G1657 blend is observed upon the application of microwave treatment/heating. The as-cast morphology of G1657 is characterised by a 1st order peak at 0.219 nm^{-1} with a broad shoulder at 0.427 nm^{-1}, which is ascribed to spheres exhibiting liquid-like short range order (LSO).[54] Upon annealing of G1657, the first order peak shifts from 0.219 to 0.235 nm^{-1} and gets significantly sharper along with the emergence of two higher order peaks at 0.412 and 0.468 nm^{-1}, with the peak positions in q/q^* ratio of 1:√3:2, characteristic of a morphology consisting of hexagonally packed spheres.[8]

The findings demonstrate that for the BCP systems investigated here, with a small molecule acting as a microwave interacting species, the amount of energy introduced, and any consequent morphological development, is independent of the sample environment and is solely a function of the level of microwave interactive species present in the polymer film. This is clearly very different to the case in thermal annealing where the amount of energy transferred to a system depends upon the temperature of the sample environment. This approach should therefore be capable of "selective" annealing, where the thermal processing/morphology optimisation of a multicomponent composite systems could be controlled through the selective localisation of a microwave absorber, where the entire system is microwave treated/heated and annealing only occurs selectively at locations where the microwave absorber is located.

In order to demonstrate selective polymer annealing, a simple bilayer composite was fabricated consisting of a layer of G1652 and a layer of G1657 + DEGDB (where both layers are placed on top of each other shown schematically in Figure 3a right). Our hypothesis was that when the composite is microwave treated only the layer containing the microwave interactive species (G1657 + DEGDB) will exhibit morphological development. In such a two-component system the obtained radially integrated scattering pattern will be a convolution of the two separate polymer morphologies. G1657 was chosen to be the doped material containing a microwave interacting species, due to its (relatively) large shift in the position of the first order scattering peak upon annealing (that was most pronounced for 6 wt% loading of DEGDB). Thus, if this material undergoes selective annealing, a clear shift in a scattering peak would be observed, as opposed to a refinement/sharpening of any features (as observed for G1652).

In situ SAXS profiles of the bilayer polymer system containing G1657 + G1652 with 6 wt% DEGDB are presented in Figure 3. The data show that the two peaks at 0.205 and 0.412 nm^{-1}, associated with the lamellae-forming G1652 remain unchanged upon microwave treatment/heating. By comparison, a shift in the peak from 0.157 to ~0.234 nm^{-1} is observed in the first 10 minutes of the microwave treatment/heating process, is attributed to morphological development of G1657 containing 6 wt% DEGDB [*N.B.* split peaks for the bilayer system are observed at low *q* due to non-uniformities arising as a consequence of the (relatively) slow casting process]. The selectivity of the structural development is most prominent in Figure 3b, which shows the evolution of the 1D SAXS profiles for the bilayer system [G1657 + 6 wt% DEGDB:G1652 (black)] and the corresponding single film systems [{G1657 + 6%DEGDB (green)} & {G1652 (purple)}]. The data clearly show that the lamellae features correlate perfectly with those observed for G1652 and do not appear to shift in any dramatic way, whilst the emergence of a peak at 0.234 nm^{-1} correlates with structural development of G1657. Comparative thermal annealing controls for the bilayer system are shown in the ESI Figure S5 and show that when the same bilayer system

comprising (G1657 + 6 wt%DEGDB):G1652 was thermally annealed, significant changes were observed in the scattering features of *both* the G1657 and G1652 copolymers.
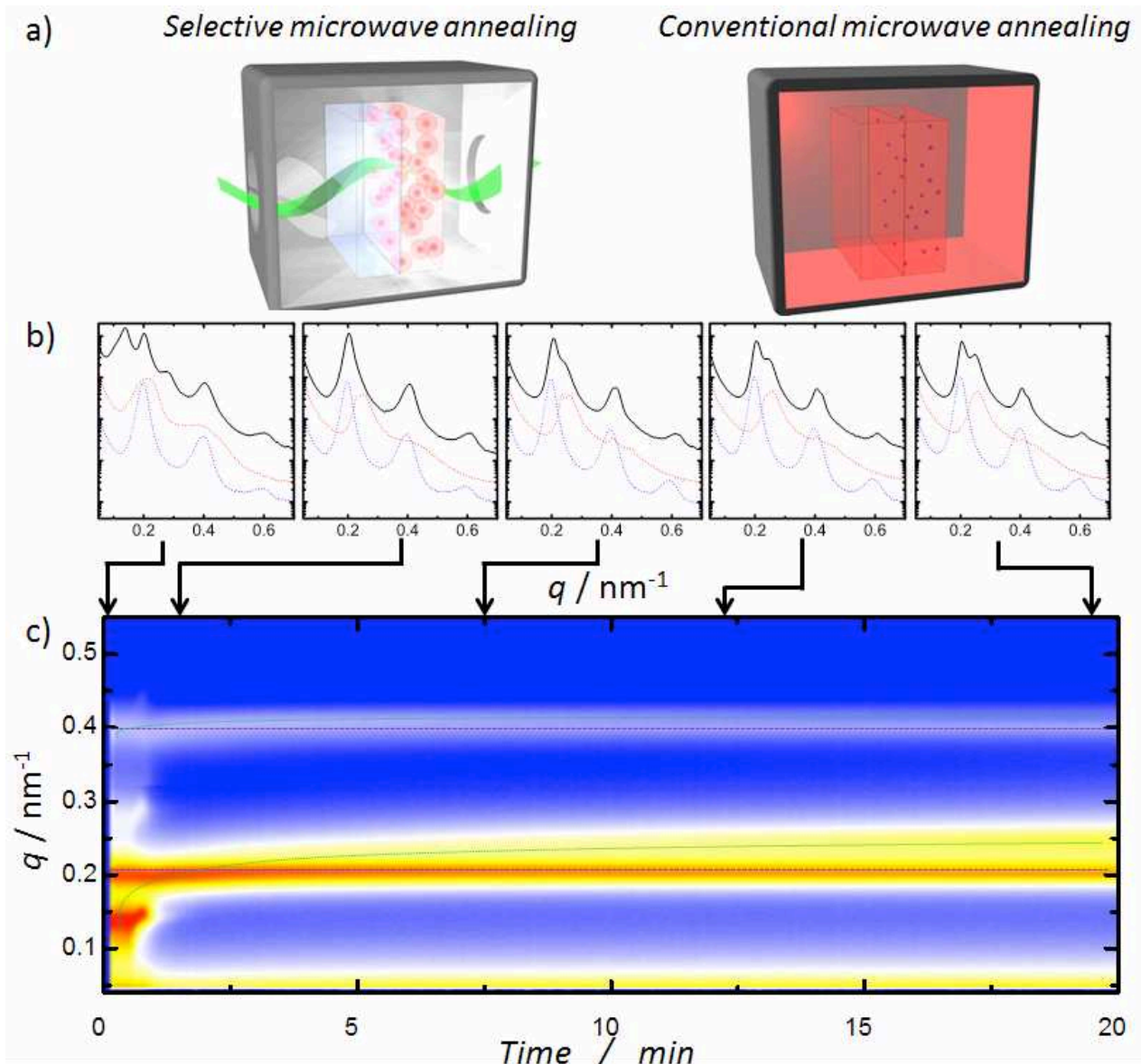

Figure 3: Selective microwave annealing of a bilayer film comprising G1652 (layer 1) with G1657 + 6 wt% DEGDB (layer 2), where (a) schematically shows the selective microwave (left) and conventional thermal (right) annealing approaches (b) shows 1D radially integrated SAXS data for the bilayer film (black) with comparative single layers films G1657 +6 wt% DEGDB (red) and un-doped G1652 (blue) at various microwave annealing times (as indicated by arrows), with curves offset along the logarithmic intensity axis for clarity and (c) shows a 2D intensity chart of 1D radially integrated SAXS data as a function of time for the bilayer film, with green and purple lines overlaid to indicate the evolution of the dominating scattering peaks arising from G1657 and G1652, respectively.

In summary, this work has developed a highly novel experimental environment that has enabled the first *in situ* observations of nanostructural development that occurs when BCPs are subjected to microwave treatment/heating. This pioneering experimental technique has been used to demonstrate how a small molecule microwave interactive additive may be incorporated as a either homogenous or localised species, directly within the BCP material which enables the usually microwave unresponsive polymeric material to interact with microwave energy, resulting in heating and consequent annealing of the BCP nanostructure. This new approach circumvents the drawbacks associated with substrate and solvent microwave annealing approaches that restrict applications beyond thin-films. Furthermore, the spatial partitioning of microwave interactive species provides new methodologies for selectively controlling the development of BCP nanostructures, opening routes for the optimisation individual components of a system independently from other elements within a complex two or three dimensional structure.

Supporting information

Supplementary figures are available in the Electronic Supplementary Information (ESI).

References

1. R. A. Farrell, N. T. Kinahan, S. Hansel, K. O. Stuen, N. Petkov, M. T. Shaw, L. E. West, V. Djara, R. J. Dunne and O. G. Varona, *Nanoscale*, 2012, **4**, 3228-3236.
2. J. Arias-Zapata, S. Böhme, J. Garnier, C. Girardot, A. Legrain and M. Zelsmann, *Advanced Functional Materials*, 2016.
3. J. N. Albert and T. H. Epps, *Materials Today*, 2010, **13**, 24-33.
4. P. D. Topham, A. J. Parnell and R. C. Hiorns, *Journal of Polymer Science Part B: Polymer Physics*, 2011, **49**, 1131-1156.
5. S. Forster and M. Konrad, *Journal of Materials Chemistry*, 2003, **13**, 2671-2688.
6. M. Matsen and F. S. Bates, *Macromolecules*, 1996, **29**, 1091-1098.
7. L. Leibler, *Macromolecules*, 1980, **13**, 1602-1617.
8. K. E. Sohn, K. Kojio, B. C. Berry, A. Karim, R. C. Coffin, G. C. Bazan, E. J. Kramer, M. Sprung and J. Wang, *Macromolecules*, 2010, **43**, 3406-3414.
9. B. Heck, P. Arends, M. Ganter, J. Kressler and B. Stühn, *Macromolecules*, 1997, **30**, 4559-4566.
10. D. A. Hajduk, P. E. Harper, S. M. Gruner, C. C. Honeker, G. Kim, E. L. Thomas and L. J. Fetters, *Macromolecules*, 1994, **27**, 4063-4075.
11. C. Cummins, P. Mokarian-Tabari, P. Andreazza, C. Sinturel and M. A. Morris, *ACS applied materials & interfaces*, 2016, **8**, 8295-8304.
12. G. H. Fredrickson and E. Helfand, *The Journal of chemical physics*, 1987, **87**, 697-705.
13. R. D. Groot and T. J. Madden, *The Journal of chemical physics*, 1998, **108**, 8713-8724.
14. J.-H. Choi, Y. Ye, Y. A. Elabd and K. I. Winey, *Macromolecules*, 2013, **46**, 5290-5300.
15. P. D. Topham, J. R. Howse, C. J. Crook, A. J. Gleeson, W. Bras, S. P. Armes, R. A. L. Jones and A. J. Ryan, *Macromolecular Symposia*, 2007, **256**, 95-104.
16. P. D. Topham, J. R. Howse, C. M. Fernyhough and A. J. Ryan, *Soft Matter*, 2007, **3**, 1506-1512.
17. H. Erothu, J. Kolomanska, P. Johnston, S. Schumann, D. Deribew, D. T. Toolan, A. Gregori, C. Dagron-Lartigau, G. Portale and W. Bras, *Macromolecules*, 2015, **48**, 2107-2117.
18. L. Wang, P. D. Topham, O. O. Mykhaylyk, H. Yu, A. J. Ryan, J. P. A. Fairclough and W. Bras, *Macromolecular rapid communications*, 2015, **36**, 1437-1443.
19. T. H. I. Epps and R. K. O'Reilly, *Chemical Science*, 2016, **7**, 1674-1689.
20. C. Park, J. Yoon and E. L. Thomas, *Polymer*, 2003, **44**, 6725-6760.
21. U. Jeong, H. H. Lee, H. Yang, J. K. Kim, S. Okamoto, S. Aida and S. Sakurai, *Macromolecules*, 2003, **36**, 1685-1693.
22. H. Ogawa, M. Takenaka, T. Miyazaki, A. Fujiwara, B. Lee, K. Shimokita, E. Nishibori and M. Takata, *Macromolecules*, 2016, **49**, 3471-3477.
23. M. W. Matsen, *Current Opinion in Colloid & Interface Science*, 1998, **3**, 40-47.
24. L. Wang, P. D. Topham, O. O. Mykhaylyk, J. R. Howse, W. Bras, R. A. Jones and A. J. Ryan, *Advanced Materials*, 2007, **19**, 3544-3548.
25. W. A. Phillip, M. A. Hillmyer and E. L. Cussler, *Macromolecules*, 2010, **43**, 7763-7770.
26. T. Thurn-Albrecht, R. Steiner, J. DeRouchey, C. M. Stafford, E. Huang, M. Bal, M. Tuominen, C. J. Hawker and T. P. Russell, *Advanced Materials*, 2000, **12**, 787-791.
27. S. Kim, G. Jeon, S. W. Heo, H. J. Kim, S. B. Kim, T. Chang and J. K. Kim, *Soft Matter*, 2013, **9**, 5550-5556.
28. Y. S. Jung and C. A. Ross, *Advanced Materials*, 2009, **21**, 2540-2545.
29. Y. Lin, A. Boker, J. He, K. Sill, H. Xiang, C. Abetz, X. Li, J. Wang, T. Emrick, S. Long, Q. Wang, A. Balazs and T. P. Russell, *Nature*, 2005, **434**, 55-59.
30. I. P. Campbell, C. He and M. P. Stoykovich, *ACS Macro Letters*, 2013, **2**, 918-923.
31. A. Knoll, A. Horvat, K. Lyakhova, G. Krausch, G. Sevink, A. Zvelindovsky and R. Magerle, *Physical Review Letters*, 2002, **89**, 035501.

32. I. W. Hamley, *Progress in Polymer Science*, 2009, **34**, 1161-1210.
33. D. Borah, M. T. Shaw, J. D. Holmes and M. A. Morris, *ACS Applied Materials & Interfaces*, 2013, **5**, 2004-2012.
34. D. Borah, R. Senthamaraikannan, S. Rasappa, B. Kosmala, J. D. Holmes and M. A. Morris, *ACS Nano*, 2013, **7**, 6583-6596.
35. P. Mokarian-Tabari, C. Cummins, S. Rasappa, C. Simao, C. M. Sotomayor Torres, J. D. Holmes and M. A. Morris, *Langmuir*, 2014, **30**, 10728-10739.
36. X. Zhang, K. D. Harris, N. L. Y. Wu, J. N. Murphy and J. M. Buriak, *ACS Nano*, 2010, **4**, 7021-7029.
37. C.-W. Chang, M.-H. Chi, C.-W. Chu, H.-W. Ko, Y.-H. Tu, C.-C. Tsai and J.-T. Chen, *Rsc Advances*, 2015, **5**, 27443-27448.
38. M. J. Kamaruddin, G. Dimitrakis, N. T. Nguyen, S. W. Kingman, E. Lester, J. P. Robinson and D. J. Irvine, *Green Chemistry*, 2011, **13**, 1147-1151.
39. M. J. Kamaruddin, N. T. Nguyen, G. A. Dimitrakis, E. R. Binner, S. W. Kingman, E. Lester, J. P. Robinson and D. J. Irvine, *Rsc Advances*, 2014, **4**, 5709-5717.
40. K. Adlington, G. J. Jones, J. El Harfi, G. Dimitrakis, A. Smith, S. W. Kingman, J. P. Robinson and D. J. Irvine, *Macromolecules*, 2013, **46**, 3922-3930.
41. C. Jin, J. N. Murphy, K. D. Harris and J. M. Buriak, *ACS Nano*, 2014, **8**, 3979-3991.
42. T. Higuchi, M. Shimomura and H. Yabu, *Macromolecules*, 2013, **46**, 4064-4068.
43. W. Bras, I. Dolbnya, D. Detollenaere, R. v. Tol, M. Malfois, G. Greaves, A. Ryan and E. Heeley, *Journal of Applied Crystallography*, 2003, **36**, 791-794.
44. R. I. Blackwell and K. A. Mauritz, *Polymer*, 2004, **45**, 3457-3463.
45. H. H. Lee, R. A. Register, D. A. Hajduk and S. M. Gruner, *Polymer Engineering & Science*, 1996, **36**, 1414-1424.
46. J. P. A. Fairclough, C. L. O. Salou, A. J. Ryan, I. W. Hamley, C. Daniel, W. I. Helsby, C. Hall, R. A. Lewis, A. J. Gleeson, G. P. Diakun and G. R. Mant, *Polymer*, 2000, **41**, 2577-2582.
47. B. Heck, P. Arends, M. Ganter, J. Kressler and B. Stühn, *Macromolecules*, 1997, **30**, 4559-4566.
48. A. Ganguly, A. K. Bhowmick and Y. Li, *Macromolecules*, 2008, **41**, 6246-6253.
49. A. D. Smith, E. H. Lester, K. J. Thurecht, S. W. Kingman, J. El Harfi, G. Dimitrakis, J. P. Robinson and D. J. Irvine, *Industrial & Engineering Chemistry Research*, 2010, **49**, 3011-3014.
50. R. J. Meredith, *Engineers' handbook of industrial microwave heating*, IET, 1998.
51. E. Lester, S. Kingman, C. Dodds and J. Patrick, *Fuel*, 2006, **85**, 2057-2063.
52. A. Metaxas and R. Meredith, *London,(UK)*, 1983.
53. D. Jones, T. Lelyveld, S. Mavrofidis, S. Kingman and N. Miles, *Resources, conservation and recycling*, 2002, **34**, 75-90.
54. J. K. Kim, H. H. Lee, S. Sakurai, S. Aida, J. Masamoto, S. Nomura, Y. Kitagawa and Y. Suda, *Macromolecules*, 1999, **32**, 6707-6717.